

The Nature of Active Sites on Zeolites

III. The Alkali and Alkaline Earth Ion-Exchanged Forms

JOHN W. WARD

From the Union Oil Company of California, Union Research Center, Brea, California

Received September 15, 1967; revised October 25, 1967

The infrared spectra of pyridine adsorbed on the alkali and alkaline earth cation forms of Y zeolite have been studied. Pyridinium ion, characterized by an infrared band at 1545 cm^{-1} , is a measure of the Brönsted acidity and coordinately bound pyridine, with an absorption band at 1451 cm^{-1} , is a measure of Lewis acidity. None of the zeolites studied exhibits Lewis acidity if the calcination temperature is less than 500°C . At 650°C calcination temperature, Lewis acidity is observed. The alkaline earth forms are Brönsted acids whereas the alkali cation forms are not. The population of Brönsted acid sites increases with decreasing cation radius and increasing electrostatic potential and field. The divalent cation forms also have structural hydroxyl groups. The electrostatic potential or field due to the divalent cation dissociates adsorbed water, producing MOH^+ and structural hydroxyl groups. The hydroxyl groups are the Brönsted acid sites. Pyridine is also coordinately bonded directly to the cation; the strength of the bonding increases with cation field for both the alkali and alkaline earth cation forms.

The variation of catalytic activity with cation was also examined. Catalytic activity is greatest for the small divalent cations for both cumene and hexane conversion. The Brönsted acidity, hydroxyl group concentration, and catalytic activity vary in a parallel manner with cation size. The acidic hydroxyl groups are similar to those of hydrogen Y zeolite and are considered to be the active sites.

INTRODUCTION

The catalytic properties of ion-exchanged zeolites have recently received considerable attention. From investigations of various cation-exchanged forms (1,2) it has been concluded that electrostatic fields associated with the cation are the seat of activity. It has also been suggested that the structural hydroxyl groups are not the active centers and that catalytic activity does not decrease with decreasing hydroxyl content (3). These reports suggest that the active sites on crystalline aluminosilicates are considerably different from those on amorphous aluminosilicates. Lewis acid sites have also been suggested as the active centers (4). On the other hand, several workers have suggested that acidic hydroxyl groups are the centers of activity (5-8).

In a previous paper (8), it was shown that there is a correlation for the hydrogen Y

zeolite between the hydroxyl group content, Brönsted acidity, and cracking activity for cumene. No relationship between Lewis acidity and catalytic activity was found. Infrared spectral studies of the chemisorption of pyridine showed that the Brönsted acidity was due to the hydroxyl groups, in particular the hydroxyl groups responsible for the 3640-cm^{-1} absorption band.

This paper extends the study to the alkali and alkaline earth cation forms of Y zeolites.

EXPERIMENTAL

Materials. The composition of the sodium Y starting material was Na 10.3%, $\text{SiO}_2/\text{Al}_2\text{O}_3$ ratio 4.9. The nitrogen surface area was $901\text{ m}^2\text{g}^{-1}$. X-Ray diffraction examination showed the sample to be highly crystalline. The cation-exchanged forms were prepared by exchange with excess 10% aqueous solutions of the desired cation

TABLE I
ANALYSIS OF SAMPLES

| | % Na | Surface area (m ² g ⁻¹) | % Exchanged |
|--------|-------|---|-------------|
| Li | 1.87 | 826 | 81.7 |
| Na | 10.24 | 901 | — |
| K | 0.02 | 899 | 99.8 |
| Rb | 1.09 | — | 89.4 |
| Cs | 2.22 | 937 | 78.3 |
| Mg (1) | 2.3 | 801 | 77.5 |
| Mg (2) | 4.9 | 810 | 52.1 |
| Ca | 0.66 | 810 | 93.6 |
| Sr | 1.09 | 810 | 89.4 |
| Ba | 1.48 | 876 | 85.6 |

nitrate at 80°C. The exchanged material was washed with distilled water to free it from residual salt. The degree of ion exchange was determined by analysis for sodium by flame spectrometry. Analyses are given in Table I. Magnesium and calcium hydrogen Y were prepared by ion exchange of ammonium Y zeolite (8) with the appropriate cation until a concentration equivalent to 40% of the exchange capacity was reached.

Pyridine was Allied Chemical Research Grade. The heart-cut was collected after distillation from sodium hydroxide and dried over 4A molecular sieve. It was further purified by the freeze-pump-thaw technique.

Apparatus and sample preparation. For spectroscopic studies, the samples were lightly ground with an agate mortar and pestle. Thin wafers, 1 inch in diameter, were prepared by compacting 0.03 to 0.07 g of zeolite in a metallurgical die under 20,000 psi. The thickness ranged from 5 to 10 mg cm⁻². The samples transmitted about 10% of the incident infrared energy. Infrared spectra were recorded using either a Cary-White 90 or a Perkin Elmer 221G spectrophotometer. The spectral resolution was about 3 cm⁻¹ and the scan speed 1 cm⁻¹/sec. The infrared cell was similar to that of Parry (9) except that CaF₂ windows were used in the place of NaCl windows and the furnace section of the cell was made from quartz. The cell could be attached to a conventional vacuum system. Vacua of 10⁻⁵ to 10⁻⁶ mm were maintained in the dynamic

system. Sample calcinations and dosings with reagents were carried out with the cell attached to the vacuum system. The cell could be inserted in the spectrophotometer reproducibly. A simple evacuated gas cell was placed in the reference beam which was suitably attenuated by screening.

Technique. The sample wafers were placed in the furnace end of the cell and evacuated. The temperature was raised to 110°C over 30 min and held until a vacuum of 10⁻⁴ mm was obtained. The temperature was then slowly raised to 500°C and maintained during evacuation for 6 hr. The sample was cooled to room temperature and its spectrum was recorded. Excess pyridine was adsorbed on the sample (i.e., sufficient to leave a small residual pressure of pyridine in the gas phase) and allowed to equilibrate for 2 hr. The spectrum of the adsorbate-adsorbent system was recorded. Further spectra were recorded as the pyridine was desorbed at a series of progressively increasing temperatures. In some experiments the pyridine was adsorbed at 110°C. Results were identical to those obtained by room-temperature adsorption. In some cases the samples were also studied after calcination at 650°C.

Catalytic activity measurements were made in a flow microreactor at atmospheric pressure. A helium carrier gas was used at the flow rate of 50 cc/min. The helium was passed through a saturator containing cumene at 20°C. The reactor was a 2-cc Vycor bulb and contained 1 g of catalyst in the form of 20-mesh granules supported on quartz wool. Analysis of feed and product streams was made by gas chromatography using a 1-m column filled with a 20% mixture of 60% Silicone Fluid 96 and 40% Carbowax 20M supported on 60-80 mesh Chromosorb W. The column was maintained at 125°C. Conversions were measured after at least 16 hr on stream. At this time, the system had reached equilibrium. No detectable loss of zeolite structure was observed after the activity test.

Thermogravimetric analyses were recorded in flowing helium with a temperature program of 1°C min⁻¹ using an Aminco Thermograv instrument.

RESULTS

The spectra in the hydroxyl-stretching region of several of the cation forms of the Y zeolite after calcination at 500°C for 12 hr are shown in Fig. 1. For the particular sample of Y zeolite studied, no absorption bands due to hydroxyl groups were observed for the alkali cation forms of the zeolite. The alkaline earth forms of the zeolite exhibited distinct hydroxyl absorption frequencies, which depended markedly on the

TABLE 2
FREQUENCIES (cm^{-1}) OF RESIDUAL OH GROUPS
ON Y SIEVES^a

| | |
|----|---|
| Li | 3700–3300 broadband removed by 350°C |
| Na | 3600–3300 broadband removed by 300°C |
| K | 3600–3300 broadband removed by 300°C |
| Rb | 3650–3300 broadband removed by 250°C |
| Cs | 3700–3200 broadband removed by 250°C |
| Mg | 3739(w), 3690(w), 3645(s), 3530 (broad) |
| Ca | 3739(w), 3688(w), 3642(s), 3582, 3520 |
| Sr | 3739(w), 3691(w), 3645(s), 3560(m), 3480(w) |
| Ba | 3750–3000 broadband removed by 400°C |

^a s, strong; m, medium; w, weak.

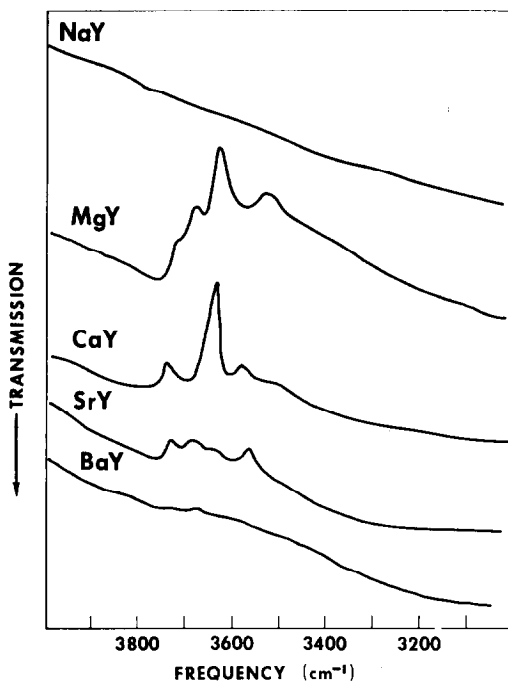


Fig. 1. Spectra of hydroxyl groups on various cationic Y zeolites after calcination at 500°C.

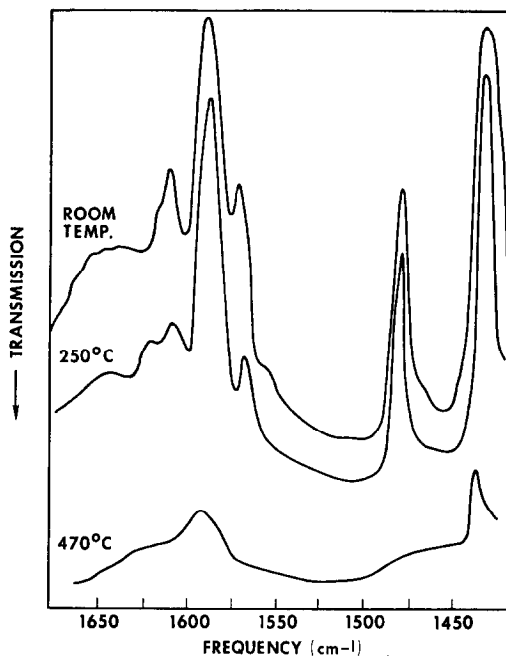


Fig. 2. Spectra of pyridine on NaY zeolite after evacuation at various temperatures.

cation. The frequencies are tabulated in Table 2 and are similar to those reported by Angell and Schaffer (10). However, with their sample of zeolite, they observed hydroxyl bands for the alkali cation forms. This difference is probably due to different origins of the zeolite. The observed differences in relative intensities of the hydroxyl bands for the alkaline earth zeolites compared to Angell and Schaffer are probably due to different origins, and minor differences in exchange and calcination conditions. Analogous to Angell and Schaffer's observations, all the hydroxyl groups could be exchanged with heavy water at room temperature.

The spectrum of adsorbed pyridine was observed both after addition of excess pyridine and after evacuation at a series of increasing temperatures for all the alkali and alkaline earth cation-exchanged forms of Y zeolite except beryllium. Typical spectra in the 1700–1400 cm^{-1} are shown in Figs. 2, 3, and 4. Figure 2 shows the pyridine adsorbed on NaY and its desorption at several temperatures. Figure 3 shows the calcium form. Figure 4 compares spectra, after evacuation at 250°C, of chemisorbed pyridine on sodium, magnesium, and barium. The mag-

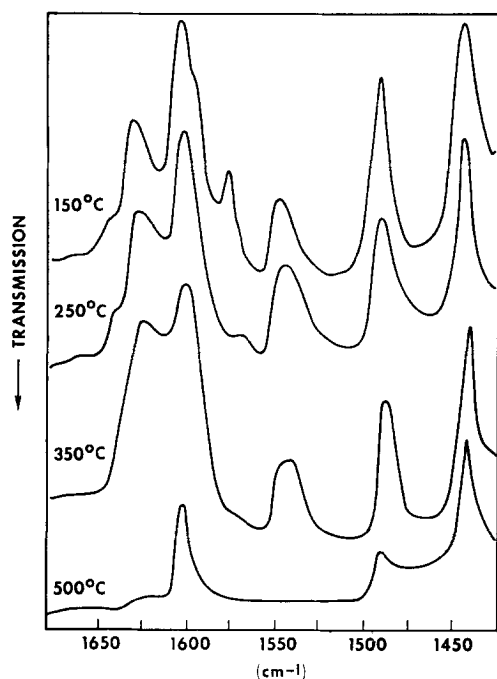


FIG. 3. Spectra of pyridine on CaY zeolite after evacuation at various temperatures.

nesium and barium represent the extreme cases for the alkaline earth cations. Little difference, apart from the precise band frequencies were observed for the alkali cations. Table 3 lists the frequencies of the observed bands between 1700 and 1400 cm^{-1} after evacuation at 250°C.

In Fig. 5, representative spectra for adsorbed pyridine are illustrated by sodium and calcium Y zeolites. The spectra shown are those of the calcined zeolite, the calcined zeolite after adsorption of pyridine, and

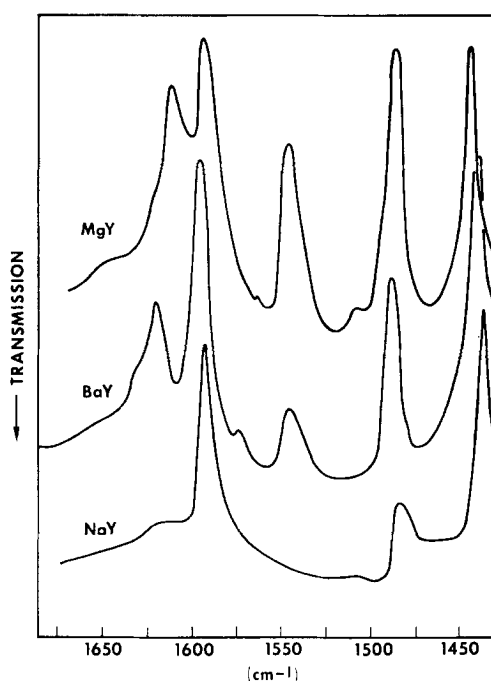


FIG. 4. Comparison of spectra in the 1700-1400 cm^{-1} region of Na, Mg, and BaY zeolites after desorption of pyridine at 250°C.

after subsequent evacuation at 250°C. The frequencies of the absorption bands after evacuation at 250°C are listed in Table 4. In the case of the calcium zeolite the hydroxyl groups are removed by adsorption of excess pyridine. However, on evacuation at 150°C for 2 hr the bands are restored with the exception of the 3688- cm^{-1} band. On evacuation at 450°C, this band is also restored. The other alkaline earth cation zeolites behaved similarly.

TABLE 3
SPECTRAL BANDS OF ADSORBED PYRIDINE BETWEEN 1700 AND 1400 cm^{-1} ^a

| Cation | Frequency |
|--------|---|
| Li | 1625(w), 1612(w), 1594(s), 1573(m), 1488(m), 1440(s) |
| Na | 1625(w), 1610(w), 1588(s), 1570(w), 1492(m), 1438(s) |
| K | 1635(w), 1605(m), 1590(s), 1575(m), 1485(m), 1436(s) |
| Rb | 1640(w), 1610(m), 1590(m), 1575(w), 1490(w), 1435(s) |
| Cs | 1630(w), 1595(m), 1580(m), 1485(m), 1434(s) |
| Mg | 1630(s), 1610(m), 1605(s), 1580(m), 1545(s), 1487(s), 1446(s) |
| Ca | 1630(w), 1615(m), 1601(s), 1575(w), 1545(s), 1490(s), 1443(s) |
| Sr | 1630(w), 1620(s), 1595(s), 1570(m), 1545(m), 1490(s), 1441(s) |
| Ba | 1630(w), 1615(m), 1590(s), 1572(w), 1545(m), 1485(s), 1439(s) |

^a s, strong; m, medium; w, weak.

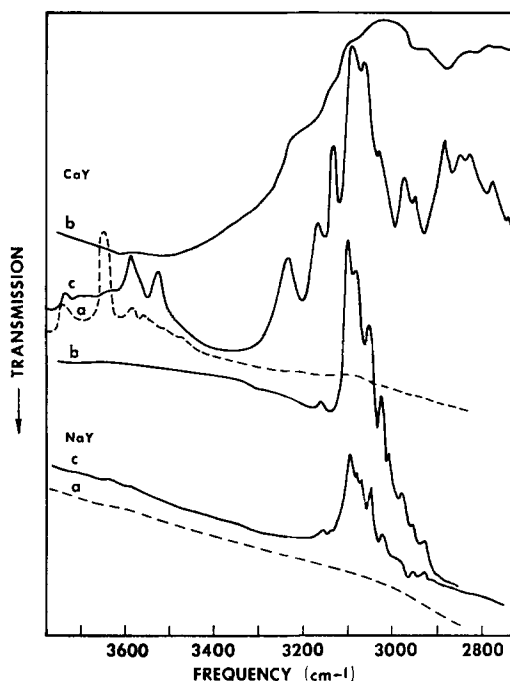


Fig. 5. Spectra of NaY and CaY zeolite in the 4000-2800 cm^{-1} region: (a) calcined at 500°C; (b) excessive pyridine adsorbed; (c) evacuation at 250°C.

Data for the conversion of cumene and hexane over the various zeolites are given in Table 5. The decomposition went cleanly to benzene and propylene. No propane was detected. Data is also listed in Table 5 for cumene cracking and hexane conversion taken from the literature (1).

Figure 6 shows thermogravimetric analyses for sodium Y and calcium Y zeolites obtained in flowing helium. These curves

TABLE 5
ACTIVITY DATA FOR CATALYTIC REACTIONS

| Sieve | % Conversion of cumene at 260°C | % Conversion of cumene at 450°C | Temp. (°C) for hexane conversion (5%) |
|-------|---------------------------------|---------------------------------|---------------------------------------|
| NaY | 0 | 8.4 | 482 |
| MgY | 68 | 99+ | 363 |
| CaY | 48 | 99+ | 422 |
| SrY | — | 79 | 428 |
| BaY | — | 49 | 472 |
| MgHY | 96 | — | — |
| HY | 96 | — | — |

show that the physically adsorbed water is removed below 300°C.

DISCUSSION

Structural Hydroxyl Groups

Differential thermal analysis, thermogravimetric analysis, and infrared spectroscopy show that physically adsorbed water is removed from Y zeolites by 250° to 300°C (Fig. 6). Any resultant infrared absorption in the hydroxyl band stretching region must then be attributed to structural hydroxyl groups. Examination of the spectra of the alkali cation Y zeolites during dehydration (Fig. 7) shows only a broad, structureless absorption band between 3700 and 3300 cm^{-1} . This band is easily removed below 350°C leaving no indication of residual hydroxyl groups. The spectra of NaY shown in Fig. 7 show this behavior and are typical of the other alkali cation Y zeolites. However, hydroxyl groups were detected on alkali cation forms which had cation defi-

TABLE 4
SPECTRAL BANDS FOR ADSORBED PYRIDINE BETWEEN 4000 AND 2800 cm^{-1} ^a

| Cation | Frequency |
|--------|--|
| Li | 3130(w), 3090(m), 3065(m), 3035(w), 2970(w) |
| Na | 3150(w), 3090(m), 3067(m), 3039(m), 3015(w) |
| K | 3150(w), 3090(m), 3060(m), 3035(m), 3005(w) |
| Rb | 3150(w), 3092(m), 3062(m), 3037(m), 3012(w) |
| Cs | 3140(w), 3090(m), 3060(m), 3040(m), 3070(w) |
| Mg | 3230(w), 3170(m), 3125(m), 3090(s), 3060(s), 3030(m), 2970(m), 2880(m) |
| Ca | 3240(w), 3170(m), 3135(m), 3095(s), 3062(s), 3040(m), 2965(m), 2880(m) |
| Sr | 3230(w), 3170(m), 3130(m), 3090(s), 3065(s), 3040(m), 2975(m), 2875(m) |
| Ba | 3240(w), 3170(w), 3127(m), 3090(s), 3065(s), 3040(m), 2970(m), 2880(w) |

^a s, strong; m, medium; w, weak.

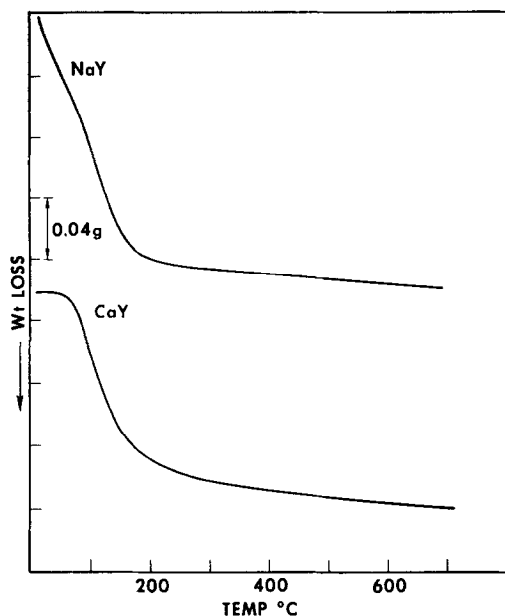


FIG. 6. Thermogravimetric analysis of Na and CaY.

ciencies. The hydroxyl groups detected by Angell and Schaffer (10) are probably, then, due to part-hydrolysis of the samples, and the zeolites with no cation deficiencies contain no detectable structural hydroxyl groups, as would be expected from considerations of the structure.

In marked contrast, the alkaline earth forms of Y zeolite, after removal of the adsorbed water exhibit infrared frequencies corresponding to structural hydroxyl groups. The frequencies are listed in Table 2. The bands near 3740, 3645, and 3540 cm^{-1} are at frequencies close to those observed for hydrogen Y zeolites (8, 12, 13, 14) while that at 3690 cm^{-1} is near that reported for Al-OH groups on X zeolites (15). The 3740-, 3645-, and 3540- cm^{-1} bands are thought to be due to Si-OH groups similar to those found on hydrogen Y zeolites and are considered to be introduced into the structure during the exchange with divalent ions. In agreement with other workers (12, 13, 14), the 3740- cm^{-1} band is believed to represent silica-type hydroxyl groups at locations terminating the giant lattice or present as impurities. The 3640- and 3540- cm^{-1} bands probably represent hydroxyl groups in or

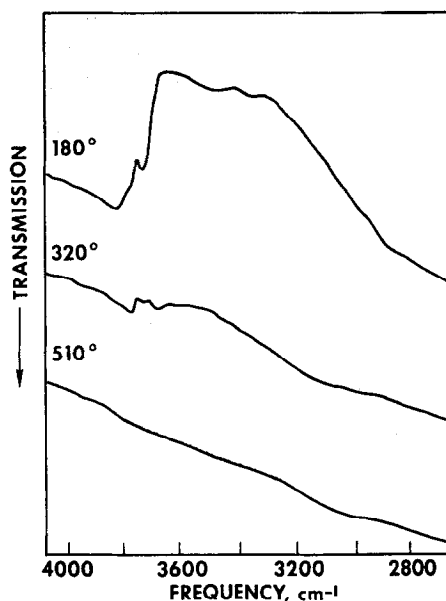


FIG. 7. Infrared spectra of NaY zeolite during dehydration.

close to one of the apertures of the supercages in the zeolite lattice.

The Nature of the Acid Sites

The use of the spectrum of chemisorbed pyridine to characterize the surface of solids has previously been reported (9, 16). Absorption bands near 3266, 3188, 3150, 1640, 1550, and 1490 cm^{-1} have been shown to be characteristic of pyridinium ions and thus are taken to be indicators of Brønsted acidity. The absorption band near 1550 cm^{-1} is the most useful for observing changes in experimental conditions on the Brønsted acidity. Absorption bands near 3150, 3120, 1620, 1580, 1490, and 1450 cm^{-1} have been attributed to coordinately bound pyridine and hence are considered to be indicators of Lewis acidity. The band near 1450 cm^{-1} is the most characteristic band for Lewis acidity observations. Furthermore, the frequency of the band near 1450 cm^{-1} has been shown, by comparison with coordination compounds, to be a measure of the strength of interaction and hence of the strength of the Lewis acid sites.

The effects on the spectra of chemisorbed pyridine by variation of the cation and the

desorption of pyridine as a function of temperature show that the nature of the zeolite is very dependent on the exchangeable cations.

On addition of excess pyridine to alkali metal cation forms, strong bands are observed in the spectrum at 3090, 3067, 3039, 3015, 1615, 1590, 1570, 1483, 1440, and 1435 cm^{-1} . For the alkaline earth forms additional bands are observed near 3260, 3170, 3140, 2980, 2826, and 1545 cm^{-1} . The region between 3100 and 2800 cm^{-1} is a region of very strong absorption with few well-defined bands (Fig. 5). The hydroxyl group bands disappear, indicating interaction of the structural hydroxyl groups with the adsorbed molecules. On evacuation at 150°C, these absorption bands of pyridine are considerably weakened or completely removed (Fig. 5), showing that physical adsorption and hydrogen bonding is occurring. The spectra of the remaining species have sharp characteristic absorption bands. Some of the hydroxyl groups are restored (Fig. 5), indicating that they were involved in hydrogen bonding. In the 1700–1400 cm^{-1} region, the main changes are the reduction in intensity of the 1577- cm^{-1} band and the removal of bands due to physical adsorption near 1440 cm^{-1} .

As illustrated by Figs. 2 to 5 and Tables 3 and 4 the spectrum of pyridine left after removal of the physically adsorbed species depends a great deal on the cationic form of the zeolite. The pyridine left after the evacuation treatment is considered to be chemisorbed.

The spectra of the alkali cation zeolites exhibit no band at 1545 cm^{-1} . No bands are observed either at 3260, 3170, or 3140 cm^{-1} (Figs. 2 and 5). It is, therefore, considered that pyridine does not chemisorb as pyridinium ions in detectable amounts on these zeolites, and hence, that they contain no Brønsted acid centers. This is expected since few, if any, hydroxyl groups were detected in the structure and no other available hydrogen is readily envisaged. However, the adsorption bands at about 1440, 1483, 1590, 1615, 3040, 3067, 3090, and 3150 cm^{-1} show the presence of coordinately bound pyridine. Table 6 shows

TABLE 6
PYRIDINE FREQUENCY AND PHYSICAL
PARAMETERS FOR VARIOUS
Y SIEVES

| Sieve | Frequency (cm^{-1}) | Ionic radius (Å) | Electrostatic field ($\text{V}/\text{Å}$) | Electrostatic potential, e/r (Å^{-1}) |
|-------|--------------------------------|------------------|---|--|
| MgY | 1446 | 0.65 | 4.9 | 3.16 |
| CaY | 1443 | 0.99 | 3.8 | 2.01 |
| SrY | 1441 | 1.13 | 3.2 | 1.77 |
| BaY | 1439 | 1.35 | 2.8 | 1.48 |
| LiY | 1440 | 0.6 | 2.1 | 1.67 |
| NaY | 1438 | 0.95 | 1.3 | 1.05 |
| KY | 1436 | 1.33 | 1.0 | 0.75 |
| RbY | 1435 | 1.48 | 0.8 | 0.67 |
| CsY | 1434 | 1.69 | 0.6 | 0.59 |
| HY | 1451 | — | — | — |

that the frequency of the band near 1440 cm^{-1} depends on the cation increasing in frequency with decreasing cation size. The plot of frequency against ionic radius is shown in Fig. 8. In Fig. 9 the band frequency is plotted against the electrostatic field strength. The field strength was calculated from the data of Rabo, Angell, Kasai, and Schomaker (3).

The plots indicate that the pyridine is more strongly held in the zeolite containing the smaller cations or stronger electrostatic field. This is confirmed by observations which show that a higher temperature is required to desorb the pyridine from the smaller cation forms than from the larger.

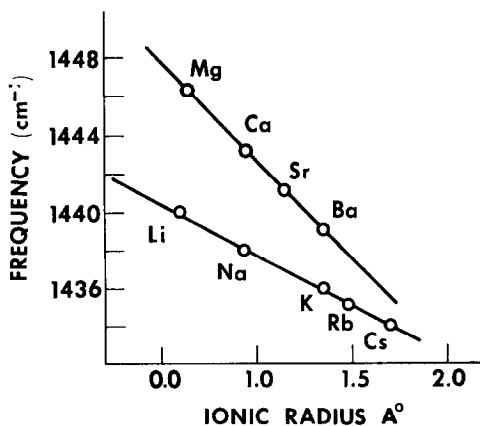


FIG. 8. Frequency of absorption band of coordinately bound pyridine versus cation radius.

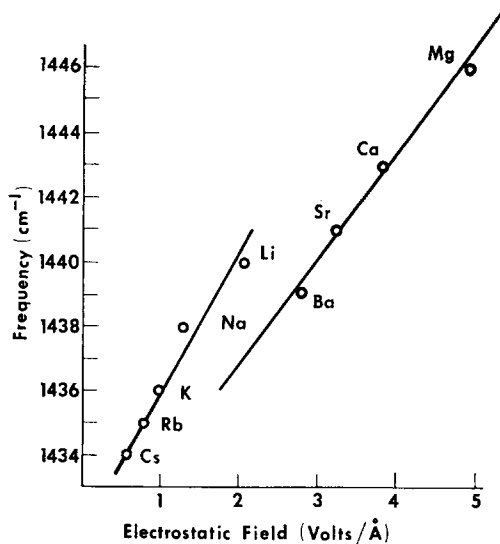


Fig. 9. Frequency of absorption band of coordinately bound pyridine on cation forms versus electrostatic field.

These results suggest that the pyridine is adsorbed by a polarization of the molecule in the field due to the cation. The interaction is probably similar to that reported for carbon monoxide (17) and carbon dioxide (18). For pyridine, the interaction probably involves the nitrogen atom. That the interaction is associated with the cation rather than being due to adsorption on Lewis acid centers (tri-coordinated aluminum atoms) is supported by the frequencies being considerably lower than those observed for pyridine chemisorbed on alumina, silica-alumina (9, 16), and the dehydroxylated hydrogen Y zeolite (8, 19). In these cases, the band is observed at 1450–1451 cm^{-1} . This assignment to adsorbate-cation interaction is supported by the adsorption of a small amount of water on the cation having no effect on the absorption band whereas for silica-alumina, Lewis sites are converted into Brönsted acid sites (20).

Similar to the alkali ions, the alkaline earth cation forms of Y zeolite all show a band attributable to coordinately bound pyridine near 1440 to 1450 cm^{-1} . Figures 8 and 9 show that there is a relationship between absorption frequency and both cation radius and electrostatic field similar to that observed for the alkali metal cation

TABLE 7
ADSORPTION OF PYRIDINE ON VARIOUS
CATION SIEVES

| Sieve | Peak height, 1545- cm^{-1} band (Sample mass) |
|--------|---|
| Mg (1) | 6.9 |
| Mg (2) | 3.4 |
| Ca | 4.3 |
| Sr | 2.5 |
| Ba | 1.5 |
| H | 15.8 |
| CaHY | 15.8 |
| MgHY | 15.8 |

forms. In general, the frequencies are higher than in the alkali cation case, showing stronger interaction presumably due to stronger fields.

In contrast to the alkali ion zeolites, the alkaline earth forms all exhibit absorption bands near 1545, 3190, and 3260 cm^{-1} which are indicative of the formation of pyridinium ion. The data of Fig. 4 and Table 7 show that the intensity of the 1545- cm^{-1} band of adsorbed pyridine and therefore the concentration of Brönsted acidity depends on the cation. Figure 10 shows that there is almost a linear relationship between the cation radius and the Brönsted acid site concentration. Figures 10 and 11 show the relationship between Brönsted acidity and electrostatic field strength and electrostatic potential. Observations on the desorption of pyridine as a

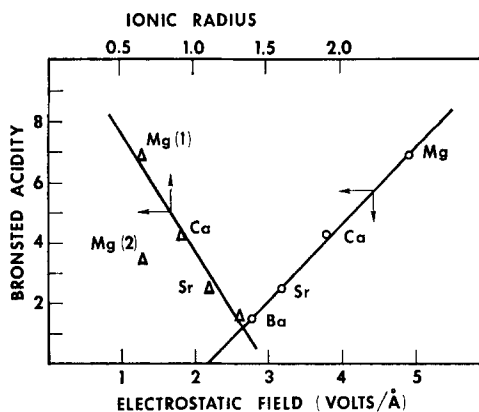


Fig. 10. Concentration of Brönsted acidity versus cation radius and electrostatic field.

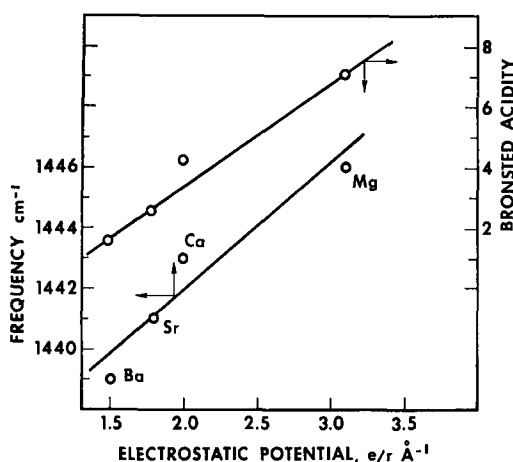


FIG. 11. Concentration of Brønsted acidity and frequency of coordinately bound pyridine versus electrostatic potential.

function of temperature indicate that the Brønsted acid sites on the various cation forms are of the same strength (20).

Hence, the introduction of divalent cations into the zeolite introduces hydroxyl groups and Brønsted acidity. Other multivalent cations, for example, nickel, cobalt, manganese, cadmium, cerium, and aluminum have similar effects (20). In the previous study of hydrogen Y zeolite (8), it was shown that the concentration of hydroxyl groups and Brønsted acidity decreased with increasing calcination temperature while the concentration of Lewis acid centers increased. It was also shown that the Lewis acid sites generated could be reconverted to Brønsted acid sites by addition of small amounts of water. It is noted above that after calcination at 500°C, the divalent cation Y zeolites exhibit Brønsted acidity and an absorption band due to coordinated pyridine near 1446–1440 cm⁻¹ and that the monovalent forms just show a band near 1440 cm⁻¹. In neither case is an absorption band observed near 1451 cm⁻¹ due to pyridine adsorbed on tricoordinated aluminum atoms, as observed for silica-alumina and alumina. Hence, it seems that after calcination at 500°C, the zeolites are not Lewis acids. However, if the Brønsted acidity of the cation forms is due to hydroxyl groups similar to those on the hydrogen form, conversion of Brønsted acid sites to Lewis acid

sites by calcination at elevated temperature would be expected. The frequencies of the absorption bands of the hydroxyl groups on the cation forms are very similar to those of the hydrogen form, which suggests similar types of hydroxyl groups. Their intensity is considerably less, which indicates a lower hydroxyl group concentration. Just as for the hydrogen form, calcination of the divalent cation forms at higher temperatures (650°C) results in a decrease in concentration of hydroxyl groups (20). Similarly, the concentration of Brønsted acidity decreases while absorption bands at 1451 cm⁻¹ are observed, indicating the formation of Lewis acid sites (Fig. 12). Similar treatment of the alkali cation forms has no effect, confirming that the band observed on these zeolites near 1440 cm⁻¹ is not due to Lewis acidity. The similarity of the hydroxyl groups on the alkaline earth and hydrogen zeolites is further confirmed by only the 3640-cm⁻¹ band type of hydroxyl groups retaining chemisorbed pyridine at 250°C. An approximate measure of the relative strengths of the pyridine-cation adsorption and the Brønsted acid sites can be obtained by studying the ease of desorption as a function of temperature. Examination of the 1440- and 1545-cm⁻¹ bands

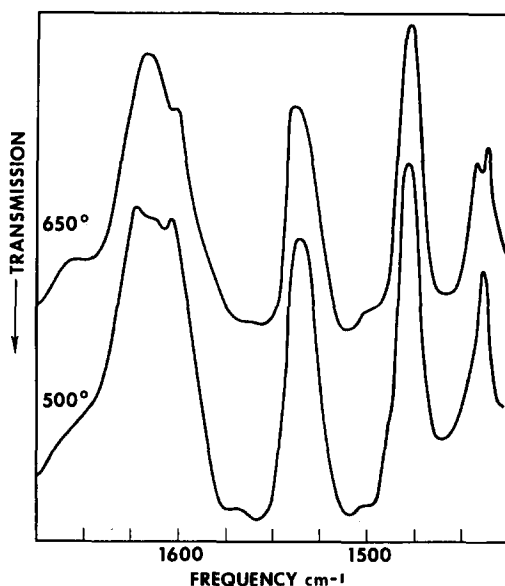
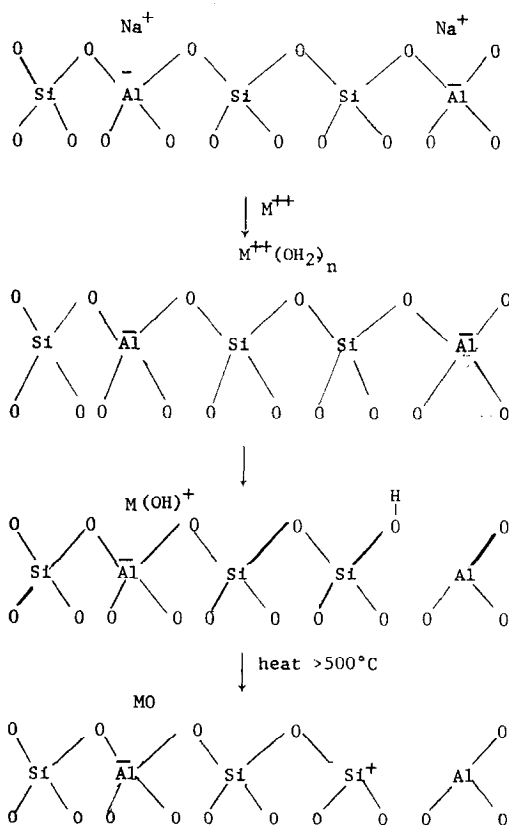


FIG. 12. Spectra of pyridine adsorbed on Y zeolite after calcination at 500° and 650°C.

shows that for calcium, the coordinately bound pyridine is most strongly retained. The same applies for the magnesium form, whereas for strontium and barium, both forms are retained with equal strengths. For the zeolites calcined at 650°C, the Lewis acid sites retain pyridine more strongly than the Brönsted acid sites. As suggested by the frequency shifts for the adsorbed pyridine, the smaller cations retain pyridine more strongly than the larger ions.

It remains now to interpret these properties in terms of the zeolite structure. Most of the phenomena can be understood if the exchange and calcination of the zeolite follows the following scheme. It is suggested that a partially hydrolyzed polyvalent ion occupies one ion exchange position and that a proton attaches to a lattice oxygen near the other position. Thus, for a divalent ion zeolite the following reactions occur:

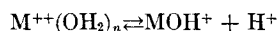


A similar hydrolytic scheme has been proposed for trivalent ions by Venuto *et al.* (25)

and Rabo *et al.* (3). Hall (27) has also proposed a hydrolytic scheme for magnesium.

Thus one structural hydroxyl group is formed for every two exchange sites. These hydroxyl groups would be similar to those presented in hydrogen Y zeolite and the cation form would, therefore, dehydroxylate at high calcination temperatures accompanied by conversion of the Brönsted acidity to Lewis acidity.

The variation of the hydroxyl content and Brönsted acidity of the various alkaline earth forms may mean that an equilibrium exists:



The small cations with their associated high electrostatic field and polarizing power would result in the equilibrium moving to the right while the larger cation would be expected to produce less dissociation.

Relationship Between Acidity and Catalyst Activity

The catalytic activity of zeolites has been attributed to Brönsted acid sites, Lewis acid sites, and electrostatic fields (2, 8). The cationic forms of Y zeolite provide a system in which the acidity and electrostatic fields can be varied in a regular manner. Hence a comparison of the catalytic activity and the acidity and electrostatic field as the cation is varied should reveal information on the nature of the active sites.

The studies of pyridine adsorption on the alkali cation Y zeolites show that these forms of zeolites possess neither Lewis nor Brönsted acidity while the alkaline earth forms possess only Brönsted acidity when calcined below 500°C. Since cumene cracks at low temperature (260°C) over alkaline earth zeolites, the reaction must be taking place on sites other than Lewis acid sites. This conclusion is supported by the previous deductions (8) which showed that for hydrogen Y zeolite, there was no relationship between Lewis acid content and toluene cracking. The data of Table 5 also show that cumene does not crack over sodium Y zeolite at 260°C. Hence Brönsted acidity or strong electrostatic fields must be necessary for carbonium ion reaction.

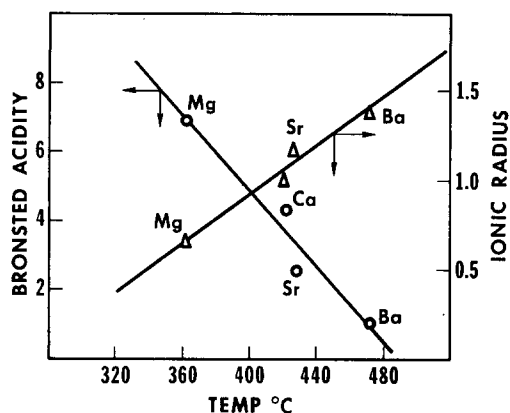


FIG. 13. Temperature for hexane conversion (5%) versus ionic radius and Brønsted acidity.

The data of Table 6 and Figs. 10, and 13 to 15 show that as the ionic radius decreases and electrostatic field and potential increase, the activity for cumene cracking at both 260° and 500°C and hexane conversion increases, showing that the cation has a considerable effect on the catalytic activity.

Examination of Table 6 and Fig. 10 shows that as the ionic radius of the cations is decreased the Brønsted acidity of the system increases in a regular manner. Figures 10 and 11 show that linear relationship exists between the electrostatic field and electrostatic potential and the Brønsted acidity. Hence the fields of the cation must have some influence on the availability of protons on the zeolite surface. Examination of Fig. 1 shows that the concentration of hydroxyl groups also increases with decreasing cation size.

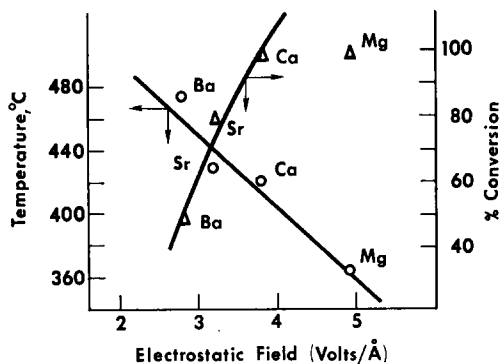


FIG. 14. Temperature of hexane conversion (5%) and cumene conversion at 500°C versus the electrostatic field strength.

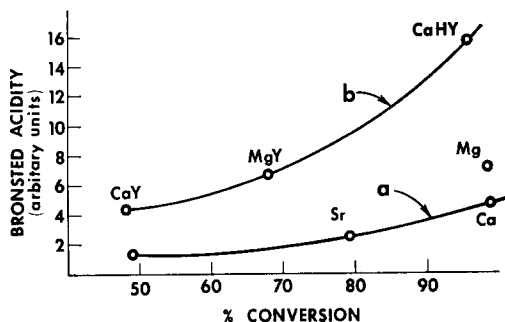


FIG. 15. Cumene conversion at (a) 500°C and (b) 260°C versus Brønsted acidity.

Figures 13 and 15 show the relationship of Brønsted acidity to cumene conversion at 260° and 450°C and the temperature for hexane conversion at a given conversion. The three curves show that the greater the concentration of Brønsted acid sites, the greater the catalyst activity. The conversion data in Fig. 10 was taken from refs. (3) and (11). From the variation of catalytic activity, Brønsted acidity, and hydroxyl group concentrations with cation, it is reasonable to conclude that the Brønsted acid sites are the active centers on the alkaline earth forms of zeolites as on the hydrogen Y form. These centers are probably generated by the polarizing action of the cation on adsorbed water resulting in dissociation as suggested above. This results in the formation of acidic hydroxyl groups similar to those on hydrogen Y zeolite. Because the maximum concentration of acidic hydroxyl groups on divalent cation zeolites cannot be greater than one-half the maximum concentration of hydroxyl groups on hydrogen Y zeolite, the catalytic activity must always be less, as found. It has been suggested by Pickert *et al.* (11) that the electrostatic field due to the cation is the seat of activity. This field is alleged to polarize the adsorbed molecules and thus induce activity. The results presented certainly show that the cation does effect the activity, and in fact, the greater the electrostatic field, the greater the activity. Similar effects in dehydrohalogenation reactions have been reported (21). However if only the cation field was responsible for the activity, it would be difficult to understand the decrease in activity with increasing

calcination temperature observed for both cracking (5) and alkylation (22) and the increase in activity on readdition of small amounts of water. Since variations in calcination temperature and rehydration are known to effect the structural hydroxyl content, these observations tend to confirm the role of acidic hydroxyl groups as active centers. Further support of the role of adsorbed water and cations is found in the work of Habgood *et al.* (23, 24). They found that the rate of the isomerization of cyclopropane increased with decreasing cation radius and was greatest for hydrogen Y zeolite. They also found that small amounts of water increased the rate of reaction. Venuto, Hamilton, and Landis (25) have also shown that the alkylation of benzene over rare earth X zeolite is enhanced by proton donors.

The role of the cation as a catalytically active site is further revealed by the studies of Miale, Chen, and Weisz (26) of the conversion of *n*-hexane over a series of different cation-exchanged zeolites. The Arrhenius plot of the observed rate constant variation with temperature suggests similar activation energies of about 30 kcal/mole on a number of different preparations in spite of large differences in relative levels of activity. These observations suggest that the active site is common to all systems and hence is not the simple cation. The common site is probably the acidic hydroxyl groups induced by the cation.

The effects of cations are also shown by the investigations of the magnesium Y zeolite at two different concentrations of magnesium, the other cation being sodium, which does not contribute to the Brönsted acidity and cracking activity. The results show that by increasing the magnesium content from 40% to 80% of the ion exchange capacity, the Brönsted acidity increases from 3.4 to 6.9 units. (Tables 1 and 7.)

It is now interesting to compare the relative contribution of Brönsted acid centers introduced via cations and those introduced by thermal decomposition of ammonium forms of sieves (8). This can be seen by comparing the cation forms, the cation-

hydrogen forms, and the hydrogen forms. This was done for the magnesium and calcium hydrogen forms, both containing 40% of the exchange capacity as divalent cation. First it is seen that the metal hydrogen forms both have about the same Brönsted acidity (15.8 arbitrary units). This suggests that in these forms the hydrogen introduced via the ammonium ion rather than via the cation is the dominating site. It is also apparent that the ammonium-derived hydrogen produces a marked increase in the Brönsted acidity—from 6.9 to 15.8 in the magnesium case and from 4.3 to 15.8 in the calcium case. A marked increase in the activity for cumene cracking is also observed—from 68% for magnesium to 96% for the magnesium hydrogen form. This compares with a change of 48% for calcium to 68% for magnesium. Furthermore, the hydrogen form derived solely from the ammonium form (1% residual sodium) gives a conversion of 96% and exhibits a Brönsted acidity of 15.8 units. Hence high activity and acidity appears to be unrelated to polyvalent cation content of the sieve. Furthermore replacement of the cations in the accessible positions by hydrogen considerably enhances the activity and acidity.

In conclusion, the acidity and activity of zeolite cracking catalysts is related to the size and type of cation. Alkali cation zeolites are nonacidic and do not catalyze carbonium ion reactions. The alkaline earth cation zeolites are Brönsted acids and active catalysts. The active sites are acidic hydroxyl groups. The cation promotes the formation of these sites by polarizing adsorbed water so that dissociation occurs. The smaller the cation, the greater is the polarizing effect.

ACKNOWLEDGMENTS

The author is grateful to Mr. Rowland C. Hansford for the catalytic activity measurements and much advice.

REFERENCES

1. PICKERT, P. E., RABO, J. A., DEMPSEY, E., AND SCHOMAKER, V., *Proc. Intern. Congr. Catal-*

- ysis, 3rd, Amsterdam, 1964* **1**, 714 (Wiley, New York, 1965).
2. PICKERT, P. E., BOLTON, A. P., AND LANEWALA, M. A., A.I.Ch.E International Symposium on Kinetics and Catalysis, Columbus, Ohio, May 1966
 3. RABO, J. A., ANGELL, C. L., KASAI, P. H., AND SCHOMAKER, V., *Discussions Faraday Soc.* **41**, 328 (1966).
 4. TURKEVICH, J., NOZAKI, F., AND STAMIREN, D. N., *Proc. Intern. Congr. Catalysis, 3rd, Amsterdam, 1964* **1**, 586.
 5. PLANK, C. J., *Proc. Intern. Congr. Catalysis, 3rd, Amsterdam, 1964* **1**, 727.
 6. VENUTO, P. B., WU, E. L., AND CATTANACH, J., Society of Chemical Industry Conference on Molecular Sieves, London, 1967.
 7. BENESI, H. A., *J. Catalysis* **8**, 368 (1967).
 8. WARD, J. W., *J. Catalysis* **9**, 225 (1967).
 9. PARRY, E. P., *J. Catalysis* **2**, 371 (1962).
 10. ANGELL, C. L., AND SCHAFFER, P. C., *J. Phys. Chem.* **69**, 3463 (1965).
 11. RABO, J. A., PICKERT, P. E., STAMIREN, D. N., AND BOYLE, J. E., *Actes Congr. Intern. Catalyse 2^e Paris, 1960*, **2**, 2055 (Editions Technip, Paris, 1961).
 12. UYTTERHOEVEN, J. B., CHRISTNER, L. A., AND HALL, W. K., *J. Phys. Chem.* **69**, 2117 (1965).
 13. EBERLY, P. E., *J. Phys. Chem.* **71**, 1717 (1967).
 14. WHITE, J. L., JELLI, A. N., ANDRE, J. M., AND FRIPIAT, J. J., *Trans. Faraday Soc.* **63**, 461 (1967).
 15. CARTER, J. L., LUCCHESI, P. J., AND YATES, D. J. C., *J. Phys. Chem.* **68**, 1385 (1964).
 16. BASILA, M. R., KANTNER, T. R., AND RHEE, K. H., *J. Phys. Chem.* **68**, 3197 (1964).
 17. ANGELL, C. L., AND SCHAFFER, P. C., *J. Phys. Chem.* **70**, 1413 (1966).
 18. WARD, J. W., AND HABGOOD, H. W., *J. Phys. Chem.* **70**, 1178 (1966); ANGELL, C. L., *J. Phys. Chem.* **70**, 2420 (1966).
 19. LIENGME, B. V., AND HALL, W. K., *Trans. Faraday Soc.* **62**, 3229 (1966).
 20. WARD, J. W., unpublished results, 1964.
 21. VENUTO, P. B., GIVENS, E. N., HAMILTON, L. A., AND LANDIS, P. S., *J. Catalysis* **6**, 253 (1966).
 22. VENUTO, P. B., HAMILTON, L. A., AND LANDIS, P. S., *J. Catalysis* **4**, 81 (1966).
 23. BASSETT, D. W., AND HABGOOD, H. W., *J. Phys. Chem.* **64**, 769 (1960).
 24. HABGOOD, H. W., AND GEORGE, Z. M., Society of Chemical Industry Conference on Molecular Sieves, London, 1967.
 25. VENUTO, P. B., HAMILTON, L. A., AND LANDIS, P. S., *J. Catalysis* **5**, 484 (1966).
 26. MIALE, J. N., CHEN, N. Y., AND WEISZ, P. B., *J. Catalysis* **6**, 278 (1966).
 27. HALL, W. K., *Chem. Eng. Progr., Symp. Ser.* **63** (No. 73), 68 (1967).